

## THE NTF AS A NATIONAL FACILITY

Oran W. Nicks

NASA Langley Research Center

As Lloyd Jones made abundantly clear in his keynote talk, the needs for high Reynolds number test capability were well established prior to the planning of a National Transonic Facility (NTF). To set the frame for the discussions to follow, some background on the activities which led to the definition of the NTF and the general agreements reached regarding its use and operations is given.

Both the Air Force and NASA began proposing high Reynolds number transonic tunnels in the late 1960's. Prominent configurations were a Ludwig tube proposed by the Arnold Engineering Development Center (AEDC), and high-pressure blowdown and continuous-flow facilities proposed by NASA. In the 1972-73 period, Langley work with cryogenic technology provided theoretical and experimental data which led to serious consideration of this approach.

In 1973 and 1974, both NASA and the USAF developed firm plans for transonic facilities. The Air Force had obtained congressional approval in the FY 75 budget for an intermittent operation high Reynolds number tunnel (HIRT) and NASA had planned for a fan-driven cryogenic transonic research tunnel (TRT) to be included in the FY 76 budget. Both the NASA and USAF tunnel projects encountered the abrupt escalation of construction costs in 1974; this consideration caused the USAF to defer construction of HIRT and the NASA to withhold the TRT from its FY 76 budget request. DOD and NASA officials then agreed to undertake an additional joint study under the cognizance of the Aeronautics and Astronautics Coordinating Board (AACB) to seek other ways for satisfying national transonic wind tunnel needs. A subpanel of the AACB was formed with a charge and membership as shown in figure 1. These members were to be supported by other NASA/DOD personnel and have involvement with industry to a significant extent. During an initial meeting on November 1, 1974, the pattern was set for a major coordinated effort involving government and industry which has continued to the present time.

One of the most significant actions of the subpanel was to develop a mission model for consideration in the selection of appropriate facilities. Thought was given to the types of aircraft which had experienced transonic problems and to a projection into the future to insure tunnel conditions capable of meeting the performance envelopes of families of military and civil aircraft. Several aircraft were selected as representing typical designs of the future. Velocity/altitude performance maps for these aircraft were then translated into maps of Reynolds number against Mach number, as indicated in figures 2 to 4. Not only were the envelopes of importance, but the cruise points were highlighted for long-range aircraft. In the case of combat aircraft, high angle-of-attack maneuvering conditions requiring small models to prevent blockage were an important consideration. For supersonic transports, the climb to cruise conditions through the transonic regime and the subsonic cruise for

overland flights were critical since as much as 30 percent of the fuel for a given mission could be expended in this period. For the hypersonic reentry vehicles, such as the space shuttle, energy management during the transonic region was extremely important to the landing footprint. It was also recognized that control loads and other aerodynamic effects caused by blunt bodies were Reynolds number sensitive and would benefit greatly from such high Reynolds number data.

Matching of wind tunnels to these requirements was possible as indicated in figure 4. Illustrated is a transport aircraft envelope with various tunnel pressures and horsepower overlaid to show portions of the flight envelope covered. This clearly allowed assessments of variations in tunnel horsepower and pressure for a given wind-tunnel size. Another illustration of this matching process for all the sample aircraft considered is shown in figure 5 for different tunnel pressures, if the same 2.5-meter-square test section and the necessary horsepower at Mach 1 are assumed. From such an approach it was possible to reach agreement on a maximum Reynolds number requirement, a test-section size, and a maximum operating pressure and horsepower required for the tunnel fan drive.

Costs were always considered as a driving factor in the facilities study. The range of cost options considered is illustrated in figure 6, with the TRT and HIRT representing thoroughly studied designs used as anchor points. The strong relationship between Reynolds number and cost is obvious.

After it appeared that the cryogenic concept offered the lowest cost approach and after the wind-tunnel size was determined, detailed studies were made of the productivity to be expected. In addition to identifying aircraft types for use in projected programs, the mission model provided estimates for the NTF use on the basis of numbers of polars per year. Although this represented a simplified basis for approximation, the approach was tested with detailed mission models and was found to be suitable for planning purposes. It was concluded that 8000 polars per year or its equivalent would form a good baseline for assumed operational cycles. It appeared that this amount of testing could be accommodated with between one and two shifts/day of operation, and also allowed for additional testing if required. Sample operating costs per year were calculated and compared with other Langley tunnels, as indicated in figure 7. The NTF estimated operating costs are highly dependent on the cost of liquid nitrogen. For these estimates, current nitrogen costs of \$70 per ton have been assumed.

Another task placed on the subpanel was the matter of considering an operating arrangement. In summary, the subpanel recommended that the NTF operation be patterned after the Unitary Plan with management at a local level under the overview of a joint NASA/DOD Board of Directors (fig. 8). It was strongly urged that both development and research users be recognized in a way to provide balance in the beneficial use of the facility. A study of the exact approach is continuing under an extended frame of reference for the subpanel.

Over a period of approximately one year, a concentrated effort led by the special AACB Subpanel resulted in a facility technical and management proposal

supported by NASA/DOD and industry spokesmen. Agreement was reached that the facility should be built at the Langley Research Center and approval was obtained through NASA, Office of Management & Budget (OMB), and the Congress for the first Fiscal Year funding. Plans are well along for the construction of the facility. It is indeed timely that you are attending this workshop to discuss the highest priority research uses for the facility in order to guarantee immediate benefit when the NTF becomes operational.

Charge:

- Redefine test requirements
- Develop low cost options
- Consider a single transonic facility - use existing hardware if feasible
- Recommend facility concept(s)
- Propose acquisition schedule

Members:

Co-chairman	B. P. Osborne - DOD	R. O. Dietz - AF
Co-chairman	O. W. Nicks - NASA	J. G. Mitchell - AF
	H. A. Morse - Army	S. L. Treon - NASA
	H. R. Chaplin - Navy	D. D. Baals - NASA

Figure 1.- 1974 AACB Subpanel for transonic facilities.

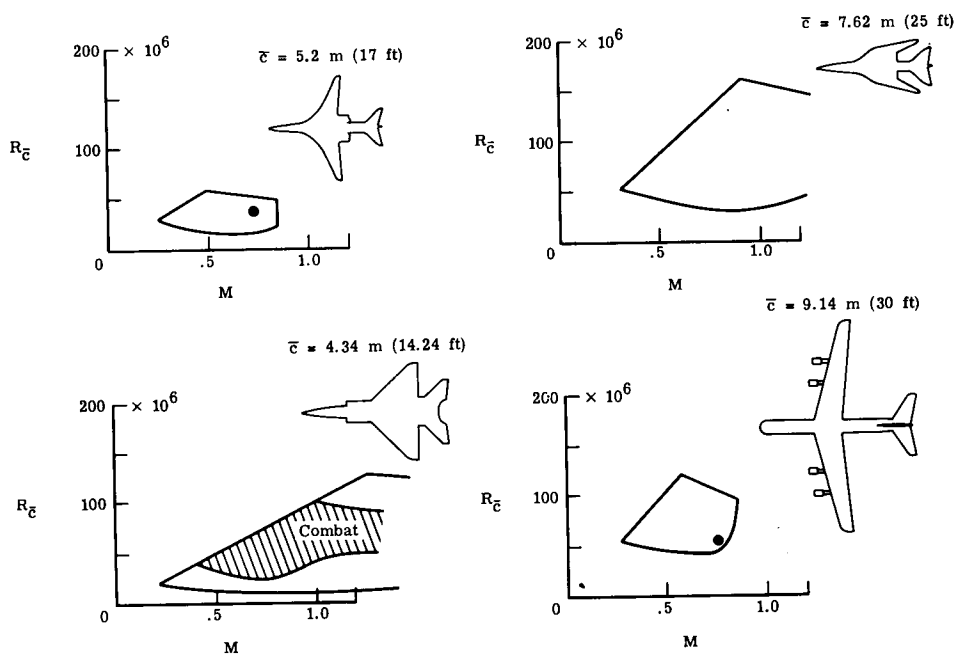


Figure 2.- Requirements for military aircraft.

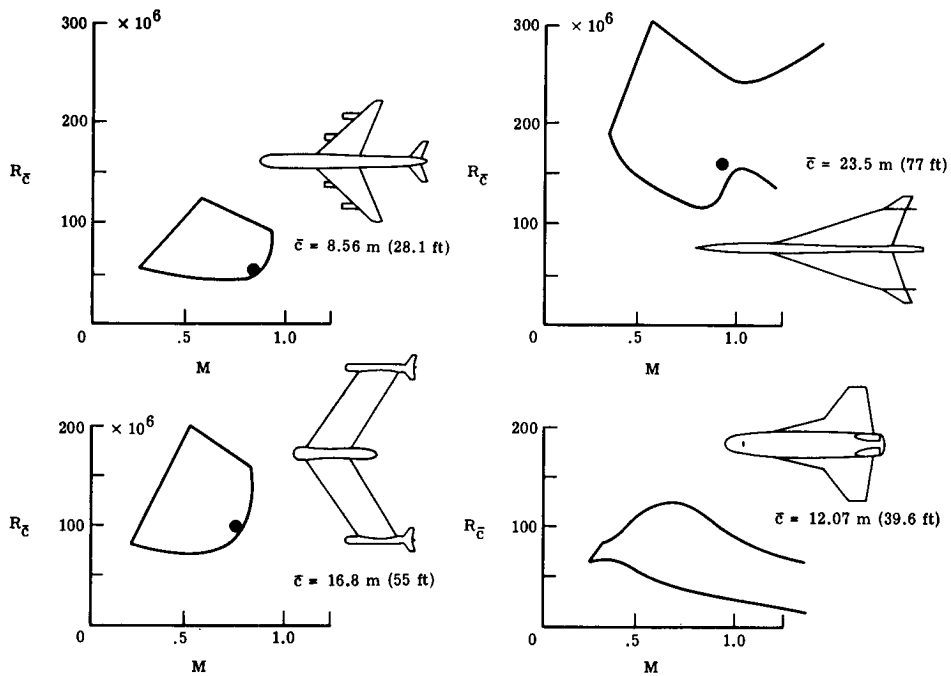


Figure 3.- Requirements for commercial aircraft.

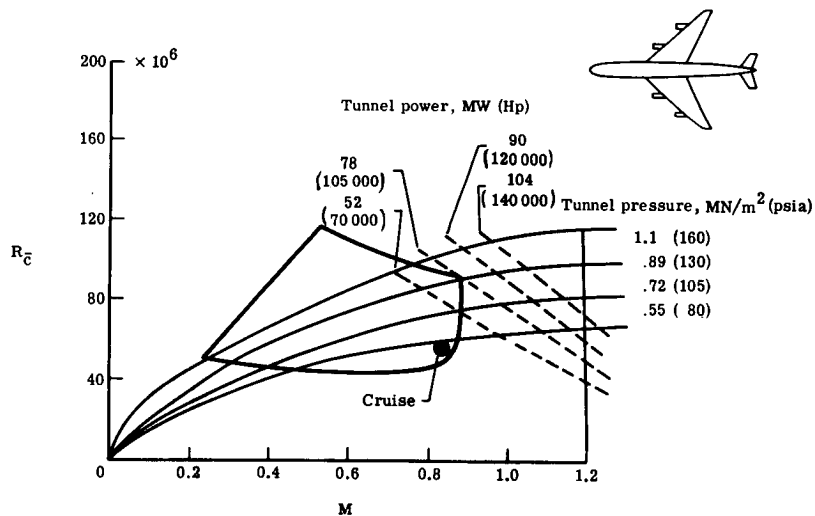


Figure 4.- Matching of transport aircraft flight performance with cryogenic wind tunnels of various pressure levels. Test section size 2.5 by 2.5 m (8.2 by 8.2 ft).

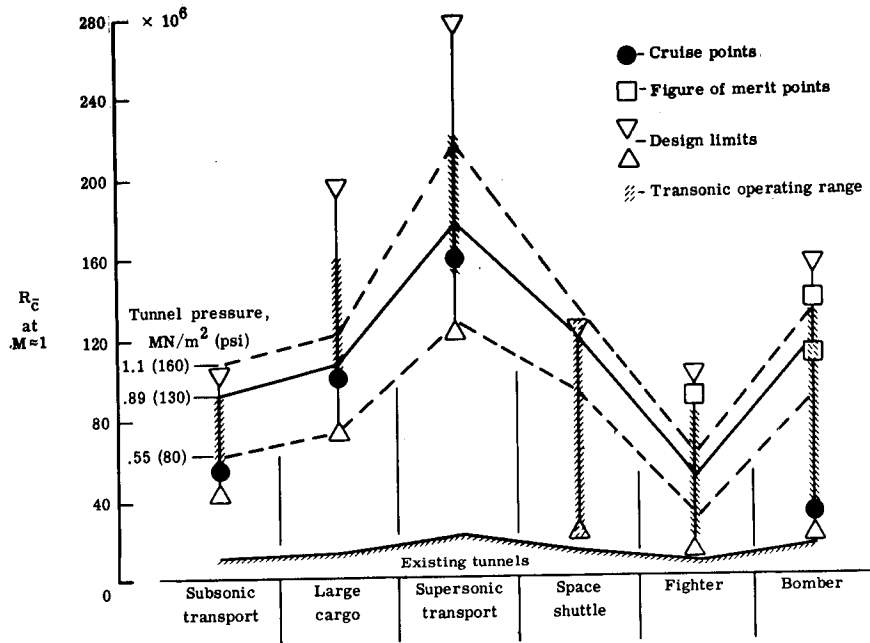


Figure 5.- Operating Reynolds numbers. Typical aircraft, 2.5 m square test section.

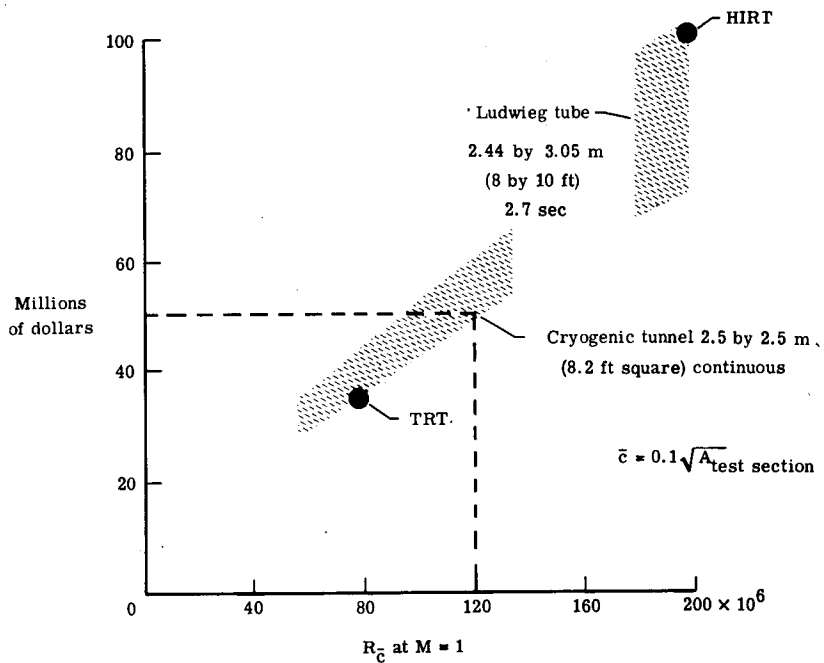


Figure 6.- Cost options considered.

	$(R_{\bar{c}})_{\max}^{(1)}$	Polars/year	Million \$/year
Langley 8-foot transonic pressure tunnel	$4 \times 10^6$	2000	0.46
Langley 16-foot transonic tunnel	$6 \times 10^6$	900	1.3
Langley Unitary Plan wind tunnel	$4 \times 10^6$	5000	1.2
National transonic facility (2.5 m)	$120 \times 10^6$	8000	5 to 10

(1)  $\bar{c} = 0.1 \sqrt{A_{\text{test section}}}$  ;  $M = 1$

Figure 7.- Operating comparison with other Langley tunnels.

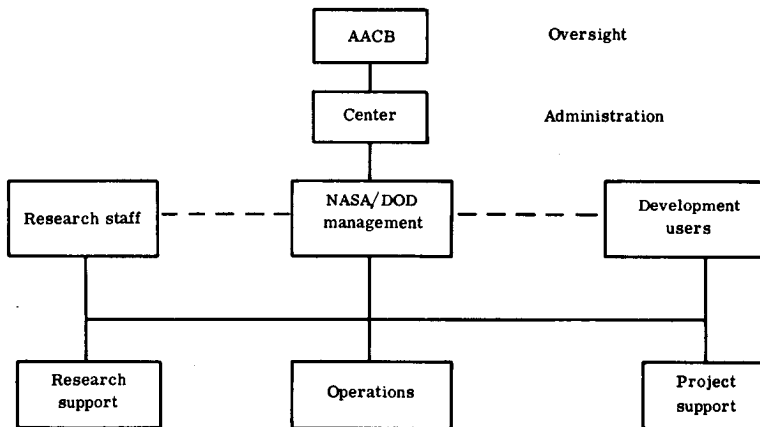


Figure 8.- Operating arrangement.

# THE U.S. 2.5-METER CRYOGENIC HIGH REYNOLDS NUMBER TUNNEL\*

Robert R. Howell and Linwood W. McKinney

NASA Langley Research Center

## SUMMARY

The U.S. 2.5-meter cryogenic high Reynolds number tunnel is a fan-driven transonic wind tunnel scheduled for operation in 1981. It will operate at Mach numbers from 0.1 to 1.2, stagnation pressures from 1 to 9 bars, and stagnation temperatures from 352 to 80 K. The maximum Reynolds number capability will be  $120 \times 10^6$  at a Mach number of 1.0 based on a reference length of 0.25 meter. This paper describes the basis for the conceptual approach, the engineering design including unique features, and the performance operating envelopes for the tunnel.

## INTRODUCTION

As man hones the perfection of his technology, his design tools must become more sophisticated. So it is with the field of aerodynamics. The continual review, both in the United States and in Europe, of our understanding in this field has identified areas where improvements in our testing and research tools will result in markedly more accurate predictions of the flight performance of full-scale vehicles. The implementation of some of the improved tools, however, involves significant capital investment.

Over the past decade, the United States has wrestled with the problems of inadequate Reynolds number in its wind tunnels, particularly for transonic aerodynamic testing. Starting in 1967, a number of different approaches have been proposed for the solution of this facility problem - most of which were prohibitively expensive. In 1974, a panel of experts was convened to review again the high Reynolds number testing requirements for the United States and make recommendations as to the criteria for a single facility to satisfy those needs. This panel worked for a period of 6 months and produced criteria and recommendations summarized in figure 1.

The cost of obtaining high Reynolds number data was a driving factor in the establishment of practical limits. Thus, this figure reflects the panel's

---

\*Paper presented at 10th Congress of International Council of Aeronautical Sciences (ICAS), Ottawa, Canada, Oct. 3-9, 1976. Reprinted by permission of ICAS.

view of the minimum acceptable criteria rather than all that was desirable. The criteria define a transonic wind tunnel (Mach range between 0.1 and 1.2) which has the Reynolds number capability at  $M = 1.0$  of  $120 \times 10^6$  based on a length equal to  $0.1 \sqrt{A_{TS}}$ . A test-section size of 2.5 meters by 2.5 meters was identified as the minimum acceptable size. Additionally, since it is viewed as a national facility and therefore required to do the necessary testing for the nation, it must have a relatively high test and data productivity. Lastly, because of the broad range of types of research and development testing envisioned for the facility, it was specified to have essentially continuous running capability (10 minutes minimum).

These criteria were accepted as guidelines for the design and construction of what is currently known as the National Transonic Facility. The National Aeronautics and Space Administration was given the responsibility for the design and construction of the facility and the Langley Research Center was selected as the site.

This paper will describe the results of the process used in selecting the facility to satisfy these requirements, and the engineering design and facility performance that has evolved.

#### SYMBOLS

A	cross-sectional area
$\bar{c}$	average wing chord
LN <sub>2</sub>	liquid nitrogen
M	Mach number
p	pressure
$\frac{\Delta p}{q}$	loss in static pressure through screen divided by dynamic pressure at the screen face
q	dynamic pressure
$R_{\bar{c}}$	Reynolds number based on average wing chord
T	stagnation temperature
$\epsilon$	turbulence level, root mean square of fluctuating velocity component

#### Subscripts

L	referenced to local conditions
SC	stilling chamber

TS test section  
T referenced to conditions in stilling chamber

## SELECTION OF APPROACH

The NASA Langley Research Center had, during the period between 1972 and 1974, established the practicality of the cryogenic approach to achieving high Reynolds numbers. (See refs. 1 to 9) As a result of their review of the experimental demonstrations of this concept, the panel endorsed the approach in their recommendations. Although the cryogenic concept would afford about a fivefold increase in Reynolds number at near atmospheric pressure (ref. 1), the concept would not meet the maximum Reynolds number criteria by itself and operation at elevated pressures was an obvious requirement. Thus, in the selection of the baseline wind-tunnel design, the leading factors considered were maximum operating pressure (which directly affected the loads on models), facility cost or capital investment, energy consumption, and productivity.

At this point, basic decisions and selection of concepts regarding the baseline facility were made. These are shown in figure 2. First, to cover the Mach range between 0.1 and 1.2, a slotted test-section approach was selected based on design and performance experience with existing tunnels; second, to satisfy the 10-minute minimum run time and to minimize energy consumption, a closed-circuit fan-drive wind-tunnel concept was selected; third, we incorporated the cryogenic approach to high Reynolds number as the only practical means available to achieving desired Reynolds number goals with manageable capital costs and model loads; and, fourth, we would require highly automated controls and data acquisition system to satisfy productivity requirements.

In reviewing this set of design concepts, it was recognized that the only really new technology that is being incorporated was the cryogenic approach to achieving high Reynolds numbers. Additional studies were made, therefore, to assure that the incorporation of this concept did not render the design impractical.

### Energy Considerations

A comparison of the cryogenic approach with the conventional fan-driven tunnel, which is recognized as the most efficient form of wind tunnel, is shown in figure 3 where the energy for 1 hour of running is presented as a function of operating (stagnation) pressure for a constant Reynolds number of  $120 \times 10^6$  at a Mach number of 1.0. For the cryogenic tunnel, the energy required is broken into that part required to drive the tunnel (electrical energy) and that required to keep the tunnel cold. In this case, cryogenic cooling is accomplished by injecting liquid nitrogen into the circuit and using it to absorb the heat of compression. There is, therefore, a continual flow of liquid nitrogen into the tunnel while it is operating. In this study, it was assumed that 1000 kWh are required to produce a ton of LN<sub>2</sub>. In the conventional tunnel, the energy is associated with the electric drive only. It is noted that for the constant Reynolds number of  $120 \times 10^6$ , the energy for the conventional wind

tunnel is considerably larger than the cryogenic tunnel at the same stagnation pressure and that the drive energy is larger than the combined drive and cooling energy for the cryogenic tunnel. Moreover, the drive energy for the cryogenic tunnel is relatively insignificant in this comparison. This fact, that the drive power required goes down with decreasing temperature, is one of the features that makes the cryogenic tunnel practical.

#### Dynamic Pressure Considerations

The impact of the cryogenic approach on dynamic pressure is shown in figure 4. In this figure, dynamic pressure is presented as a function of test-section height (assuming a square test section) for a conventional operating temperature ( $T = 320$  K) and a cryogenic temperature ( $T = 122$  K) and for a Reynolds number of  $120 \times 10^6$  at a Mach number of 1.0. It is observed that the dynamic pressure is reduced by about a factor of 4 in going from a stagnation temperature of  $T = 320$  K to  $T = 122$  K. Additionally, the test-section size required to produce a Reynolds number of  $120 \times 10^6$  is reduced by a factor of 4 by reducing the temperature from  $T = 320$  K to  $T = 122$  K. Thus, the cryogenic approach affords a more reasonable dynamic pressure as well as a more practical (less costly) facility size.

#### Variable Temperature Considerations

Another highly desirable feature of the cryogenic tunnel is that it affords temperature as a test variable. This additional test variable permits independent control of dynamic pressure and Reynolds number. A typical operating map for the cryogenic tunnel is compared with the conventional tunnel operating curves in figure 5. In the conventional fan-driven tunnel, since stagnation temperature is relatively constant, there is a fixed relationship between Mach number, dynamic pressure, and Reynolds number. Thus, as you traverse the Mach number range, model deformation (due to change in dynamic pressure) and Reynolds number also vary and it is impossible to experimentally separate these effects with a single model. In the cryogenic tunnel, because of the ability to vary temperature, the dynamic pressure (model deformation) can be held constant and Reynolds number and Mach number can be varied. Also, Reynolds number can be held constant and dynamic pressure and Mach number varied. As a consequence of this new capability, the effects of model deformation, Reynolds number, and Mach number can be completely separated. The cryogenic approach, therefore, in addition to providing practical solutions to otherwise costly requirements also affords a new research capability heretofore unavailable.

#### SELECTION OF SIZE-PRESSURE COMBINATION

Since it was clear that elevated pressure operation was required for the tunnel to keep the initial cost within bounds, an engineering consultant was hired to provide cost estimates for a series of fan-driven cryogenic tunnels scaled in size and pressure to meet a common test requirement. From these data empirical cost curves were developed (fig. 6). The cost numbers given by the curves represent U.S. dollars as of January 1975 and do not include any

contingency or escalation. The dashed line shows the various tunnel size and pressure combinations that provide  $120 \times 10^6$  Reynolds number at a Mach number of 1.0. The significant cost reduction associated with increasing the operating pressure of the tunnel for a given design Reynolds number is graphically illustrated. It is clear that the tunnel designer is forced to design for a maximum practical dynamic pressure from capital cost considerations. For the NTF, the maximum dynamic pressure was chosen as 3.3 bars at a Mach number of 1 and Reynolds number of  $120 \times 10^6$ . This resulted in a 2.5-meter-square test section and a maximum stagnation pressure of 8.96 bars.

## ENGINEERING DESIGN

The definition of the desired wind tunnel has evolved through the establishment of a set of criteria and the exercising of cost and dynamic pressure constraints. The resulting wind tunnel will have a 2.5-meter square test section, operate at pressures up to 8.96 bars, over a temperature range from 352 K to 80 K, and a Mach number range from 0.1 to 1.2. At this point, engineering design has been applied to further define the physical characteristics of the tunnel. To minimize initial costs, the NTF will be constructed on the site of the deactivated 4-foot supersonic pressure tunnel. The existing drive motors and their associated control system, as well as existing office building and cooling towers will be utilized.

### Test Section

The NTF will have a slotted test section (fig. 7) similar to the existing Langley 8-foot transonic pressure tunnel which is known to be efficient and have good quality flow. The length of the slotted region is approximately three test-section heights. The top and bottom walls have six longitudinal slots each and the wall divergence angle is adjustable to compensate for boundary-layer growth. The parallel sidewalls are fixed with two longitudinal slots in each wall. The design will allow the slot open width and edge shape to be easily modified. Remotely adjustable reentry flaps are provided at the end of each slot. The position of these flaps during tunnel operation will be programmed to control Mach number gradients through the test section and minimize power consumption. The model support system is an arc sector with a nominal travel of  $30^\circ$ . The arc sector is located downstream of the test-section reentry flaps to minimize interference effects and power consumption. The center of rotation is 3.96 meters downstream of the test-section throat. This places the model well ahead of the aft end of the test section for minimization of interference effects over the base of the model. This combination has the attendant disadvantage of making the model support sting long and creates problems particularly at the high loads which the NTF is capable of generating. Additional angle-of-attack range is provided by offset stings over a reduced load range. The sting will have a roll mechanism capable of rolling the model through  $270^\circ$ . Model pitch range is controllable in either a continuous or pitch-pause mode at rates from  $0^\circ$  to  $4^\circ$  per second.

## Contraction Ratio - Screen

The attainment of satisfactory flow quality is influenced by the contraction ratio from the stilling chamber to the test section from both a direct effect of contraction (ref. 10) and an indirect effect on antiturbulence screen design. Analysis of the data of reference 10 indicates that to achieve turbulence levels in the test section of 0.1 percent, turbulence damping screens are required. Therefore, a comprehensive analysis of screen design including the effects of contraction ratio, number of screens, wire diameter, and pressure loss through the screens was made. The results of this analysis are summarized in figures 8 and 9. The symbols on figure 8 indicate various contraction ratio-screen combinations that satisfy the turbulence requirement of 0.1 percent in the test section for an initial turbulence of 1.7 percent in the stilling chamber. (This initial level was assumed based on ref. 11.) It will be noted that the turbulence requirement is met over a range of contraction ratios from about 8 to 16. The effect of increased contraction ratio is to reduce the pressure loss through the screens which impacts the wire stresses and horsepower loss. This effect is summarized in figure 9. The symbols correspond to conditions where the test-section turbulence requirement was met in figure 8. The stresses vary from about  $415 \times 10^6 \text{ N/m}^2$  down to  $120 \times 10^6 \text{ N/m}^2$  at contraction ratios from 8 to 16 with associated horsepower losses from well in excess of 8000 down to 1000. The yield stress for 0.762 mm wire without joints is about  $520 \times 10^6 \text{ N/m}^2$ . Limited data available indicate joint efficiencies for butt-welded joints of about 70 percent. This results in a yield stress of about  $365 \times 10^6 \text{ N/m}^2$  for a screen system with joints.

Based on the considerations of adequate safety margin on wire stress and conservation of horsepower due to losses through the screens, a contraction ratio of 15 was selected for the NTF. To insure flow quality requirements can be met, up to five screens are provided for.

## Overall Tunnel Circuit

With the test-section size and the upstream contraction ratio established, the rest of the tunnel circuit layout was accomplished using near optimum conical diffusers (fig. 10). In the case of the National Transonic Facility, however, there was concern to keep the volume of the circuit as small as practical in order to keep the cost of the pressure shell within bounds and to minimize nitrogen fill costs during operation. To achieve this goal, a "rapid diffuser," an approach used in several European wind tunnels, was employed as a method of final deceleration into the stilling chamber. This method of deceleration requires a resistance in the flow at the diffuser exit equal to approximately five times the local dynamic pressure ( $\frac{\Delta P}{q} = 5$ ) to assure absence of separation.

In the current design, the resistance of a water-cooling coil is used for this purpose. This coil will be used as a heat exchanger only when the tunnel is operated at relatively high (near atmospheric) temperatures. The resistance could have been supplied by a number of other techniques.

The projected overall circuit performance in terms of compression ratio is

presented as figure 11 where the compression ratio is presented as a function of Mach number. This curve was generated by accumulating losses in the circuit including losses in the turning vanes, screens, cooling coil, test section, and diffusers. Losses include both viscous and momentum losses. The test-section loss estimate is based on experimental data obtained from a 1/5-scale model of the tunnel high-speed leg from the rapid diffuser upstream of the test section to the end of the high-speed diffuser. These data have been corrected for differences in Reynolds number. This compression ratio curve (fig. 11) has been used in defining the tunnel performance maps to be presented later.

### Test-Section Isolation System

Although the cryogenic approach using LN<sub>2</sub> has been proven to require the least capital investment and be the most energy conservative approach to high Reynolds number testing, the cost per data point for high Reynolds number tests will be considerably higher than for usual low Reynolds number data. Consequently, every step possible is being taken to conserve nitrogen which is the largest contributor to operating costs. One of the provisions made to conserve nitrogen is test-section isolation valves (fig. 12) which will be capable of isolating the test section so that the pressure can be reduced to atmospheric and personnel entry can be made to service models without venting the entire circuit.

The operation of the system requires that with the flow at rest, the contraction upstream of the test section and the high-speed diffuser downstream of the test section be disconnected from the pressure bulkhead at either end of the test-section plenum and moved away from the test section. Isolation valves are then remotely moved into the closed position and locked to the pressure bulkhead. The test section can then be vented to the atmosphere. When the pressure has been reduced to 1 atmosphere, the test-section sidewalls are lowered and work access tunnels are inserted from either side capturing the test model and sealing around the model support sting. A "shirt sleeve" work environment is maintained by fans which circulate air through the access tunnel and heaters which are used to warm the cold model to an acceptable level. After the model change or service has been completed, the process is reversed. The work access tunnels are withdrawn, the outer shell access doors are closed, the test-section walls are raised to operating position, and the pressure is equalized across the pressure bulkheads. When the pressure differential is zero, the isolation valves are remotely moved to the stored position; the contraction section and high-speed diffuser are returned to the operating position and locked to the pressure bulkheads, and the tunnel is ready to resume operation.

### Drive System

The cryogenic concept requires that the drive system be capable of producing a constant compression ratio over a large temperature range. This requirement has a major impact on the design of the drive system, since with a fixed geometry fan, the rpm required for a constant compression ratio varies as the square root of the gas temperature entering the fan. The desired

performance in the NTF will be obtained by using a single stage fan with variable inlet guide vanes and fixed outlet stators in combination with a two-speed gear box.

The fan will be driven by two existing variable speed motors (70 000 horsepower) and one inline synchronous motor (60 000 horsepower) as shown in figure 13. The two variable speed motors are on a single shaft which drives the fan through a two-speed gear box. The gear box provides the ability to match the maximum motor rpm (maximum horsepower output) to the required fan rpm at both ambient and cryogenic temperatures. The gear ratios are such that maximum motor rpm (maximum horsepower) produces fan rpm's of 600 and 360. This gear arrangement combined with the variable inlet guide vanes will provide the required constant compression ratio over the wide range of tunnel operating temperatures. The synchronous motor is on the fan shaft and, consequently, rotates at the fan shaft speed. It has a synchronous speed of 360 rpm which corresponds to the maximum speed of the variable speed motors driving through the low-speed gear. Thus, it can be brought up to speed and synchronized with the variable speed motors. In the synchronous or constant rpm operating mode, fan compression ratio (Mach number) will be controlled by use of the variable inlet guide vanes. Analytical studies have shown that the guide vanes are capable of controlling Mach number over a range between  $M = 0.6$  and  $M = 1.2$  with an acceptable level of efficiency. Below  $M = 0.6$ , the power of the synchronous motor is not required; therefore, the variable-speed capability of the existing motors can be used for Mach number control.

The power available from this system is shown in figure 14, where maximum fan-shaft horsepower is presented as a function of fan rpm. To maximize the horsepower available from the existing variable speed motors, liquid rheostats will be added to provide constant torque at rpm's down to about two-thirds of the maximum. In the high gear ratio, a maximum of 65 000 shaft horsepower is available to the fan. In the low gear ratio (used for cryogenic operation) a maximum of 125 000 horsepower is available to the fan.

#### TUNNEL PERFORMANCE

With the drive motor-gear arrangement described above, the wind-tunnel performance at selected Mach numbers of 0.8 and 1.0 are presented as figures 15 and 16. The operating maps at each Mach number are presented as stagnation pressure versus Reynolds number for varying temperatures down to the temperature where saturation of nitrogen will occur at a local Mach number of 1.4. The boundaries of the map are defined on the left by the compression ratio limit of the fan-drive system, by the available horsepower limit (125 000 horsepower) in the upper left corner, by the maximum operating pressure (8.96 bars) across the top and by the saturation boundary on the right. The tunnel will operate anywhere in the shaded region of these envelopes. The variable-speed induction motors combined with the high-speed gear cover the lower pressure range underneath the dashed line (dark shaded region). The total drive is required to cover the region above the 65 000-horsepower line. The maximum Reynolds number usually occurs where the condensation boundary intersects the shell pressure limit. This maximum Reynolds number is plotted as a function of

Mach number in figure 17. This overall maximum tunnel Reynolds number capability is bounded by the shell operating pressure limit for Mach numbers up to 1.0. Between  $M = 1.0$  and 1.2, the performance is limited by the maximum horsepower available. Above  $M = 1.2$ , the fan maximum compression ratio limits the performance. Note that the goal of a Reynolds number of  $120 \times 10^6$  for  $M = 1.0$  is achieved.

At the bottom of figure 17 is an overall envelope of the Reynolds number capability of all wind tunnels in the United States. The NTF will be capable of increasing ground-test Reynolds number by about one order of magnitude over currently existing capability.

## UNCONVENTIONAL FEATURES

### Internal Insulation

As mentioned previously, the NTF will employ in its design an internal insulation. Although internal insulation complicates the design, it affords many overriding advantages. Its principal advantage is that it minimizes the temperature excursions of the large pressure shell. In doing so, it (1) greatly reduces the liquid nitrogen required to approach steady-state operating conditions and thus reduces operating cost, (2) it minimizes the thermal stress in the pressure shell and thereby alleviates thermal fatigue as a major problem and enhances the service life of the pressure shell, and (3) it affords an opportunity to combine thermal insulation and acoustic attenuation functions into a system which will reduce the noise in the tunnel circuit. The baseline design of the insulation system (fig. 18) employs about 15 cm of fibrous insulation with perforated aluminum foil laid in at about 2.54 cm thicknesses. The aluminum foil is included to inhibit free circulation. The insulation system is enclosed by glass cloth and covered with a corrugated flow liner which is supported by tee-shaped rings welded to the pressure shell and insulated from the liner. The liner is corrugated to absorb the circumferential thermal strain. Slip joints are provided for the longitudinal movement. The tee rings are about 1.2 meters apart. Filler blocks are used under the corrugation to block flow from one insulation segment to the next. The possibility of a fire inside a pressurized wind tunnel is always a concern and a concerted effort is being made to minimize the accumulation of flammable materials. Obviously, there are a number of additional concerns such as the impact of noise on the service life of the system as well as the thermal performance of the system under a flowing cryogenic environment. These concerns are the subject of an extensive verification test program.

### Model Loads

Another somewhat unconventional feature of the NTF will be the model loads it will be capable of generating. The dynamic pressure is independent of temperature and is a function only of stagnation pressure and Mach number. In figure 19 lines of constant dynamic pressure are superimposed on the overall performance map of the tunnel. Most existing transonic wind tunnels operate at dynamic pressure levels up to about 0.5 bar. There are a few tunnels which

have dynamic pressure capability up to about 1 bar. The NTF will have a maximum dynamic pressure capability of 3.3 bars. Although the NTF, by virtue of employing the cryogenic approach, will have a much lower dynamic pressure to Reynolds number ratio as compared to the other approaches to high Reynolds number testing, it can still produce model loads of more than three times those experienced in existing wind tunnels.

Technology appears to be in hand to accommodate these loads. However, force measuring balances, sting deflections, and model deformation will tend to take on more importance as we attempt to use this new facility up to its maximum Reynolds number capability.

### Cryogenic Operation

As previously discussed, the requirement for tunnel operation at temperatures down to about 80 K requires the use of liquid nitrogen as a heat absorber. The operation utilizes the vaporization of LN<sub>2</sub> sprayed into the circuit to absorb the heat of compression of the fan. Venting of gaseous nitrogen is then required to control pressure. The operational system, figure 20, therefore, includes a bulk storage of liquid nitrogen (250 000 U.S. gal) with pumps capable of supplying liquid nitrogen at rates up to 545 kg/sec to spray nozzles in the circuit upstream of the fan, and a large vent stack to properly disperse the gaseous discharge. The vent stack poses some unusual design problems since it is required to operate over a very wide range of flow rates and pressure ratios. Additionally, it is used to provide a means of alleviating hazards associated with cold nitrogen gas both with regard to leaks in the valves and piping and from the discharge.

### Cryogenic Nitrogen Environment

Although nitrogen is the major constituent of air and is readily acceptable as an aerodynamic test gas under usual conditions, its use at cryogenic temperatures presents some unusual considerations. At cryogenic temperatures its density is high, and it can accumulate in low areas and create a hazard. To alleviate this concern, special procedures and equipment are required when the test section is opened to allow model servicing. As discussed previously, special access tunnels incorporating environmental conditioning equipment are necessary to allow personnel to enter the space around the model in a reasonable length of time. Oxygen monitors will be provided to assure breathable air (proper oxygen content).

Models for testing in this cryogenic environment will also require some extension of technology. The cryogenic temperature and higher loads will result in the selection of high strength alloy steels which have acceptable levels of ductility at cryogenic temperatures. Because of the thin boundary layer at high Reynolds number, the materials must be machinable to a very smooth finish. Methods of fastening and filling suitable for this environment are being identified.

## Productivity

The NTF is being designed to satisfy a national need for high Reynolds number test capability at transonic speeds. Moreover, as a national facility it must accommodate the projected workload of NASA, the DOD, and industrial users. As a consequence of this, as well as the need to conserve energy, the NTF is being designed to produce data at a relatively high rate. Typical existing wind tunnels produce data at about 26 000 specific sets of test conditions in a year where a set of test conditions per year is defined by a combination of Mach number, Reynolds number, angle of attack, angle of yaw, and so forth. The NTF is targeted to produce measurements at 104 000 sets of test conditions or four times the conventional rate. To achieve this goal, the tunnel control and data acquisition system will be highly automated. Computer control will be used extensively to insure optimum procedures and safety in the tunnel operation. Modern data acquisition will be provided with "quick look" data capability to minimize retesting due to improper measurements.

## INTEGRATED FACILITY

The current concept of the National Transonic Tunnel is shown in perspective in figure 21. The tunnel will be constructed on the site of the Langley 4-foot by 4-foot supersonic pressure tunnel. This tunnel will be removed and the new facility erected in its place. As mentioned previously, the NTF will make use of the existing drive motors and their drive control, the cooling tower and its mechanical equipment, and the office building. Also, as pointed out previously, the unusual features of the facility are the large liquid nitrogen bulk storage which will be used to achieve cryogenic temperatures and the large vent stack for the discharge of gaseous nitrogen to maintain constant operating pressure.

## FULL-SCALE REYNOLDS NUMBER TESTING CAPABILITY

An indication of the ability of NTF to perform the desired high Reynolds number development testing is found by assessing its ability to test at full-scale Reynolds numbers for various aircraft configurations. In figures 22 and 23, the Reynolds number capability of the NTF is compared with the flight Reynolds number of current and future aircraft. The comparison is made on the basis of Reynolds number based on the average chord of the configuration,  $R_{\bar{c}}$ .  $R_{\bar{c}}$  is presented as a function of Mach number for the flight vehicle (solid curve) and for the model in the NTF (dashed curve). The cruise point for the vehicle is indicated by the solid dot. At the bottom of each figure, the cross-hatched envelope indicates the corresponding capability of existing wind tunnels.

In sizing the models for the NTF, the span was limited to 0.6 of the width of the test section and the blockage was limited to 0.5 percent - whichever was reached first limited the model size.

In figure 22 comparisons are made for a large subsonic transport, a future supersonic transport, an advanced subsonic transport, and the space shuttle. The boundaries of the airplane flight envelope are determined by sea-level flight (upper left), flutter or buffet (upper right), thrust limitations (maximum Mach number), and maximum lift (lower boundary). The maximum lift and maximum Mach number boundaries are the more critical from aerodynamic performance considerations.

For large subsonic transports of the Boeing 747 category, the NTF will provide full-scale test conditions for the cruise point as well as for the high-speed "max q" load condition. The high Reynolds number peak at  $M = 0.6$  cannot be met by the design NTF performance envelope. This is not considered a significant deficiency, however, since the Reynolds number effects for un-separated, fully subsonic flows are usually small and predictable at high Reynolds number levels. For the advanced transport concept, such as the "span loader" in the 1.0 million kg gross weight category, the NTF can attain full-scale test conditions at the cruise point. The high-speed "max q" load condition will require the use of half-span model techniques, which are generally an acceptable approach for obtaining loads data on relatively high-aspect-ratio configurations.

For the large supersonic transport type configurations, full-scale test conditions can be attained for the subsonic cruise point ( $M = 0.95$ ). The high Reynolds number requirements at the subsonic Mach numbers ( $M \lesssim 0.5$ ) can largely be covered by the use of larger sized models, acceptable for testing at the low subsonic speeds. Full-scale test conditions for the space shuttle type configuration can be attained throughout the subsonic/transonic flight regime.

The ability of the NTF to meet full-scale testing requirements of current and advanced military aircraft is illustrated in figure 23. It will be noted that the NTF design performance envelope provides essentially full-scale test capability at subsonic/transonic speeds for a typical variable-sweep bomber in both the subsonic cruise and high-speed configurations.

The flight envelope of a typical fighter is also well covered. The cruise point for the conceptual large transport, however, falls slightly above the Reynolds number capability of the NTF. The use of the previously considered half-span model techniques, combined with limited Reynolds number extrapolation, will largely close the Reynolds number gap for this type of configuration as well as the off-design areas of the other airplane envelopes.

#### SUMMARY

In summary, this paper has described the approach being taken in the United States to achieve full-scale Reynolds numbers in a transonic wind tunnel. The facility design and planned construction represent a significant step forward in the continual requirement for new and improved research and development tools for aeronautics. It involves the incorporation of the cryogenic approach to high Reynolds number which brings full-scale Reynolds numbers

within practical reach insofar as capital costs and drive horsepower are concerned. There appear to be no insurmountable design problems. The facility is projected to be operational in 1981.

#### REFERENCES

1. Goodyer, M. J.; and Kilgore, R. A.: High Reynolds Number Cryogenic Wind Tunnel. Paper 72-995 at AIAA Seventh Aerodynamics Testing Conference (Palo Alto, California), Sept. 3-15, 1972 (AIAA J., vol. 11, no. 5, May 1973, pp. 613-619).
2. Kilgore, R. A.; Adcock, J. B.; and Ray, E. J.: Flight Simulation Characteristics of the Langley High Reynolds Number Cryogenic Transonic Tunnel. Paper 72-80 at AIAA 12th Aerospace Sciences Meeting (Washington, D.C.), Jan. 30-Feb. 1, 1974, (AIAA J. of Aircraft, vol. II, no. 10, Oct. 1974).
3. Kilgore, R. A.: The Cryogenic Wind Tunnel for High Reynolds Number Testing. Ph.D. Thesis, The University of Southampton, Feb. 1974. (Available as NASA TM X-70207.)
4. Wilson, J. F.; Ware, G. D.; and Ramsey, J. W., Jr.: Pilot Cryo Tunnel: Attachments, Seals, and Insulation. Presented at the ASCE National Structural Meeting (Cincinnati, Ohio), Apr. 22-26, 1974.
5. Ray, E. J.; Kilgore, R. A.; Adcock, J. B.; and Davenport, E. E.: Test Results From the Langley High Reynolds Number Cryogenic Transonic Tunnel. Paper 74-631 at AIAA Eighth Aerodynamic Testing Conference (Bethesda, Maryland), July 8-10, 1974.
6. Kilgore, R. A.: Design Features and Operational Characteristics of the Langley Pilot Transonic Cryogenic Tunnel. NASA TM X-72012, 1974.
7. Polhamus, E. C.; Kilgore, R. A.; Adcock, J. B.; and Ray, E. J.: The Langley Cryogenic High Reynolds Number Wind-Tunnel Program. Astronaut. & Aeronaut., vol. 12, no. 10, Oct. 1974.
8. Kilgore, R. A.; Goodyer, M. J.; Adcock, J. B.; and Davenport, E. E.: The Cryogenic Wind-Tunnel Concept for High Reynolds Number Testing. NASA TN D-7762, 1974.
9. Kilgore, R. A.; Adcock, J. B.; and Ray, E. J.: Simulation of Flight Test Conditions in the Langley Pilot Transonic Cryogenic Tunnel. NASA TN D-7811, 1974.
10. MiniLaWs Working Group: A Further Review of Current Research Aimed at the Design and Operation of Large Wind Tunnels. AGARD Advisory Report No. 83, Sept. 1975.
11. Dryden, Hugh L.; and Schubauer, G. B.: The Use of Damping Screens for the Reduction of Wind Tunnel Turbulence. J. Aeronaut. Sci., Apr. 1947.

## U.S. 2.5-METER-HIGH REYNOLDS NUMBER TRANSONIC WIND TUNNEL (NATIONAL TRANSONIC FACILITY - NTF)

- $R_{\bar{c}} = 120 \times 10^6$  AT  $M = 1.0$
- MACH NUMBER RANGE - 0.1 TO 1.2
- CONTINUOUS OPERATION (10 MINUTE MINIMUM)
- HIGH PRODUCTIVITY

Figure 1.- Basic high Reynolds number testing requirement as specified by Facilities Review Panel.

- CRYOGENIC CONCEPT\*
- SLOTTED TEST SECTION
- FAN-DRIVEN CLOSED-CIRCUIT PRESSURE WIND TUNNEL
- HIGHLY AUTOMATED CONTROLS AND DATA ACQUISITION SYSTEM

\*ONLY NEW TECHNOLOGY

Figure 2.- Approach selected to meeting high Reynolds number testing requirement.

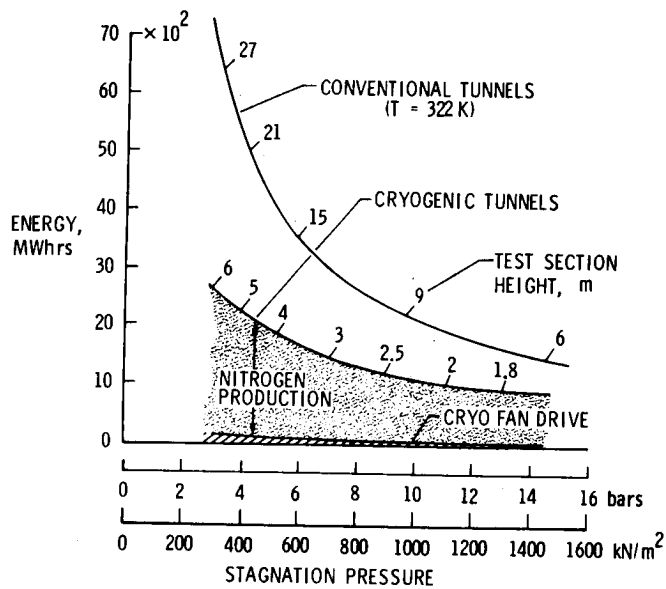


Figure 3.- Comparison of the energy consumed in 1 hour of operation for conventional and cryogenic tunnels,  $R_{\bar{c}} = 120 \times 10^6$ ;  $M = 1.0$ ;  $\bar{c} = 0.1$  test section height.

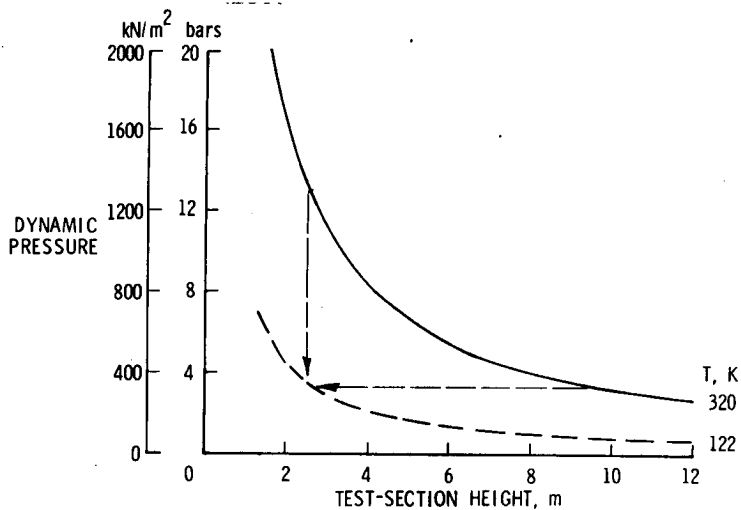


Figure 4.- Effect of cryogenic temperature on dynamic pressure and test-section size.  $R_{\bar{c}} = 120 \times 10^6$ ;  $M = 1.0$ ;  $\bar{c} = 0.1$  test-section height.

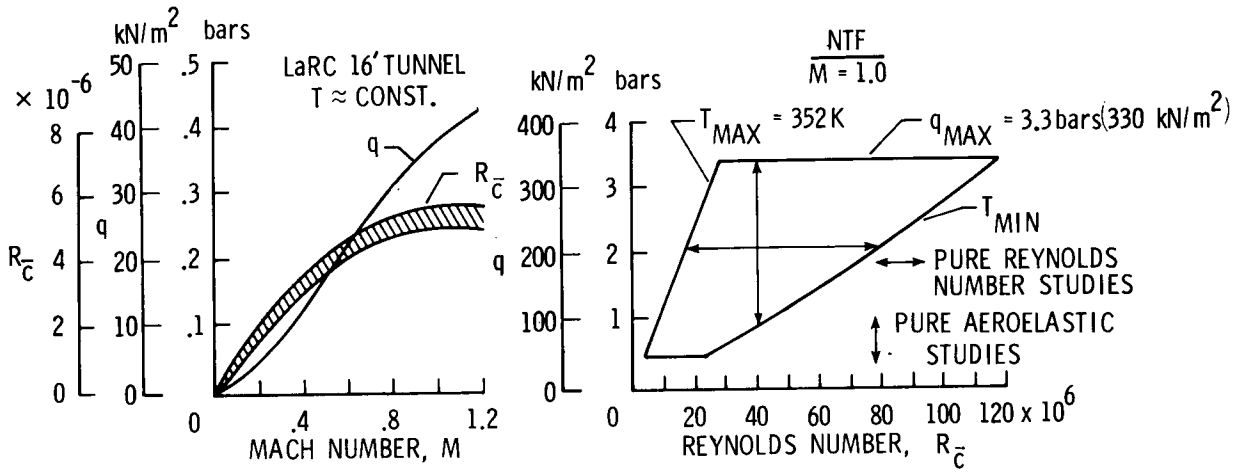


Figure 5.- The impact of having temperature as a test variable on research test capability.

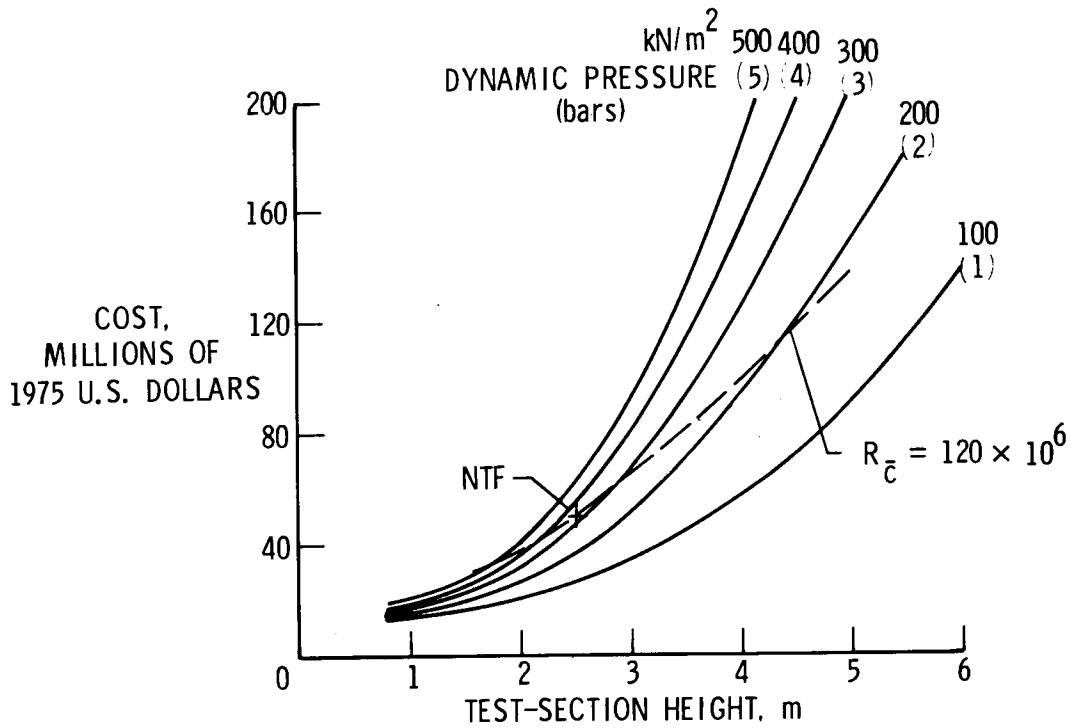


Figure 6.- Variation of tunnel cost with test-section size and dynamic pressure,  $M = 1.0$ ;  $T = 122\text{ K}$ .

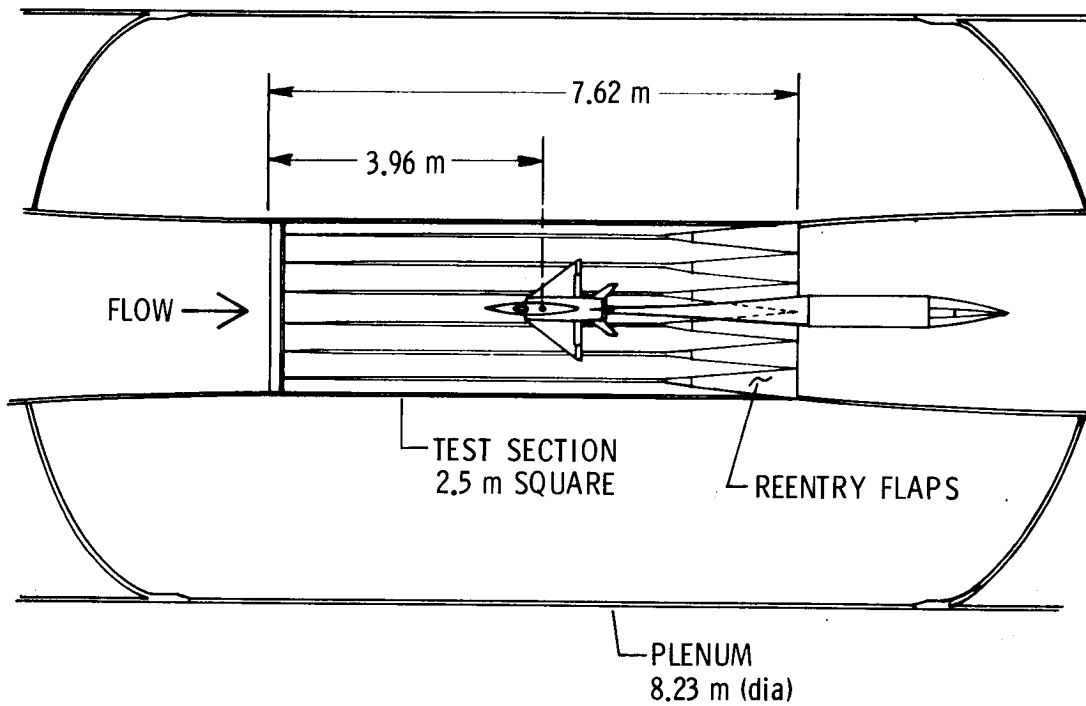


Figure 7.- Plan view of the slotted test section.

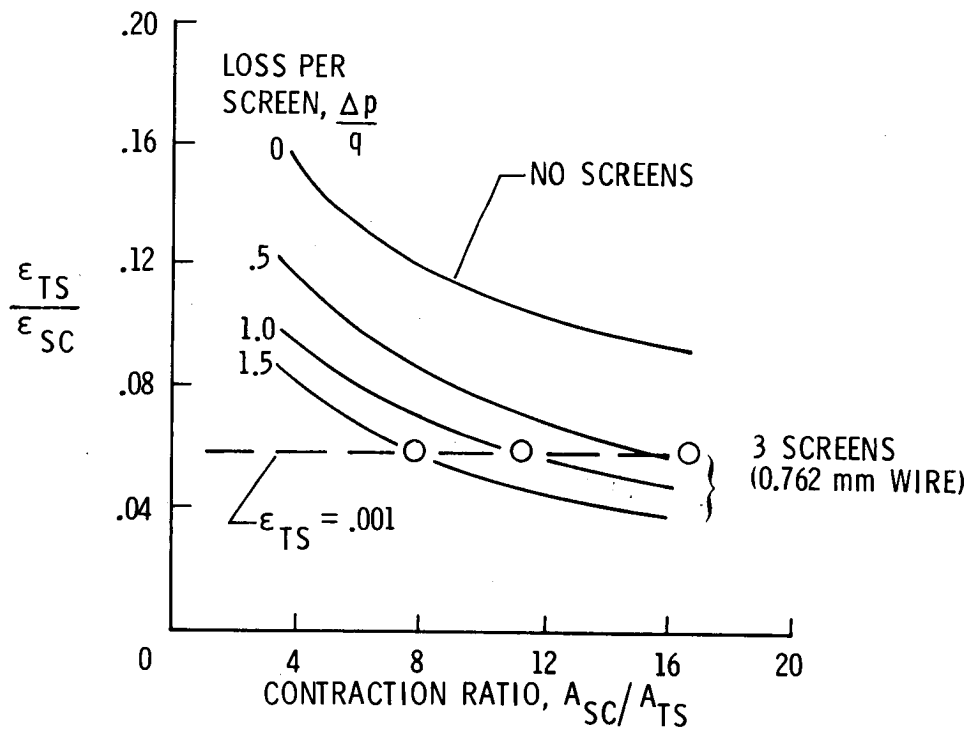


Figure 8.- Effect of contraction and screens on turbulence attenuation.  
 $M = 1.0$ ;  $\epsilon_{SC} = 0.017$ .

WIRE STRESS, MN/m<sup>2</sup>

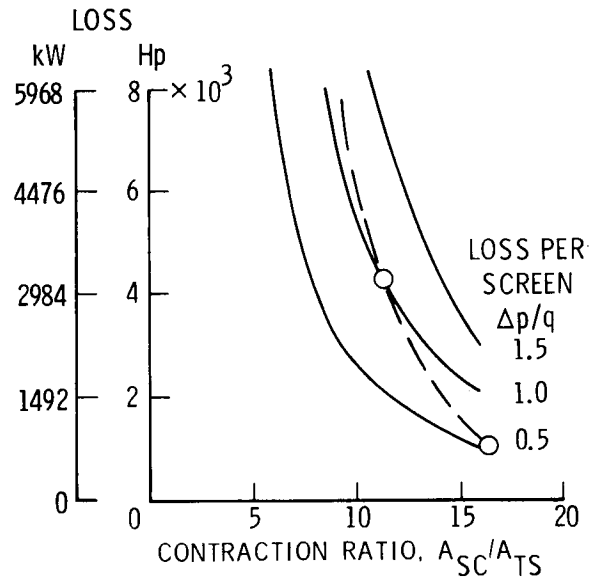
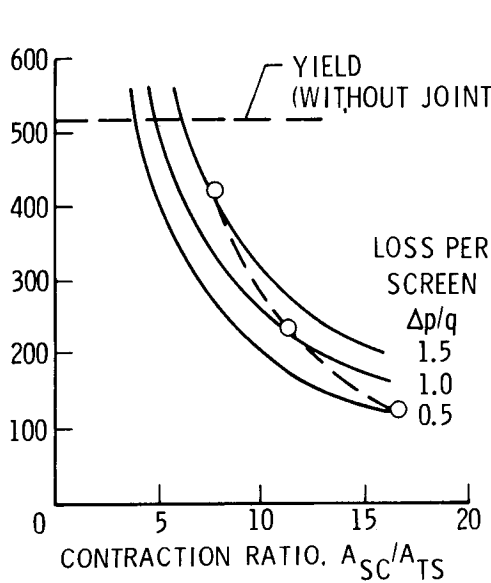


Figure 9.- Effect of contraction ratio on screen stress level and screen loss for three levels of screen pressure drop. Three screens; 0.76 mm wire diameter;  $p_t = 896 \text{ kN/m}^2$  (8.96 bars); 0.61 m sag.

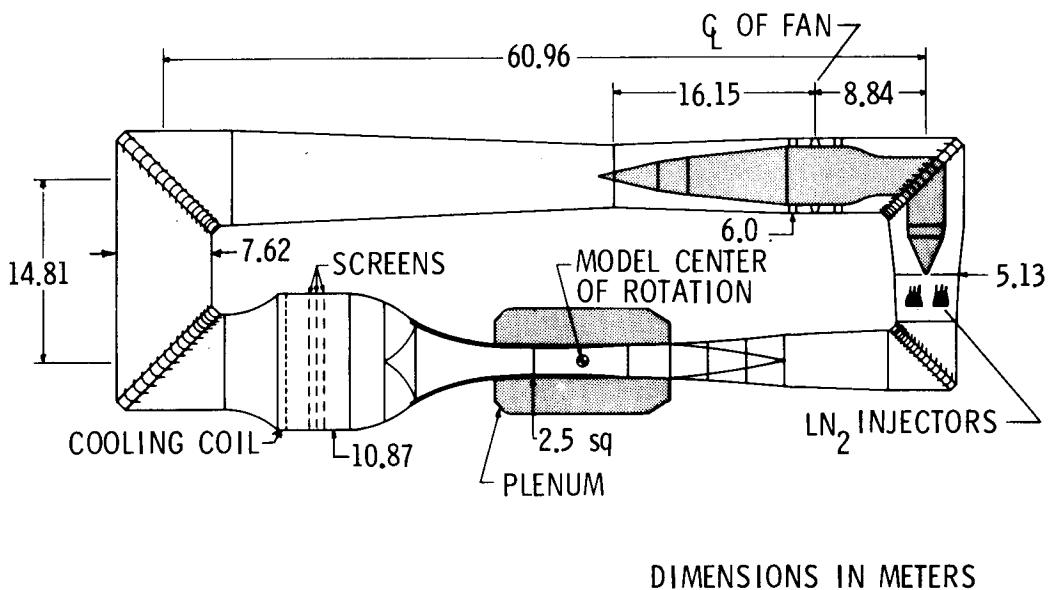


Figure 10.- Lines of the aerodynamic circuit of the National Transonic Facility.

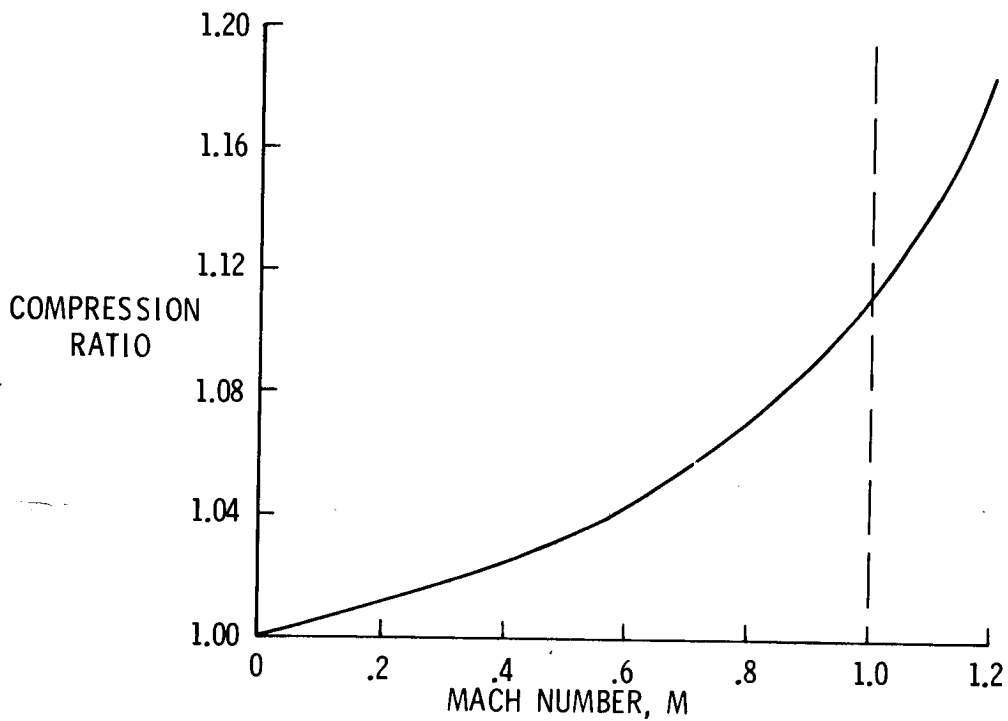


Figure 11.- Compression ratio required to drive the National Transonic Facility as a function of Mach number.

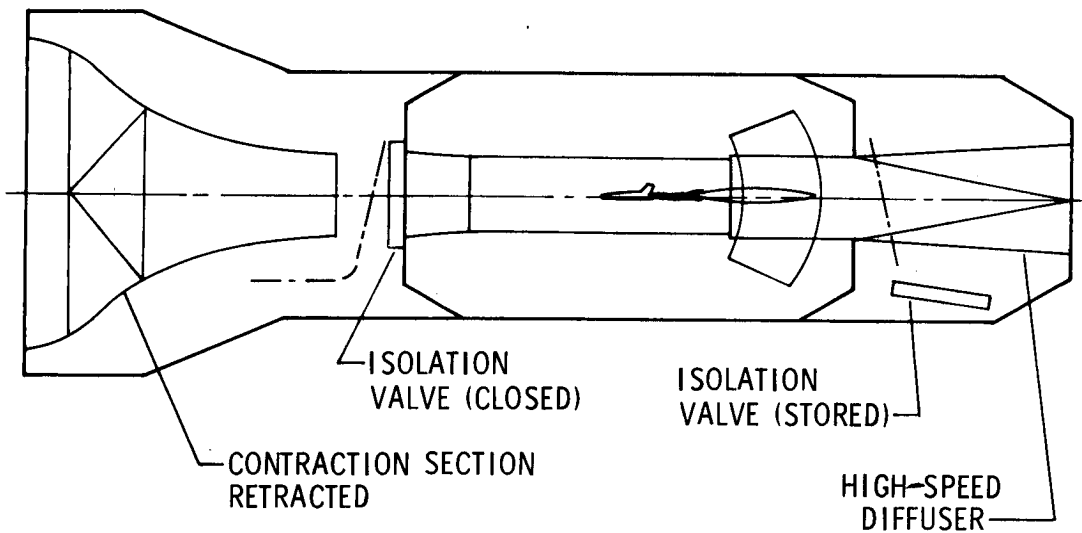


Figure 12.- Schematic of the test-section pressure isolation system for the National Transonic Facility.

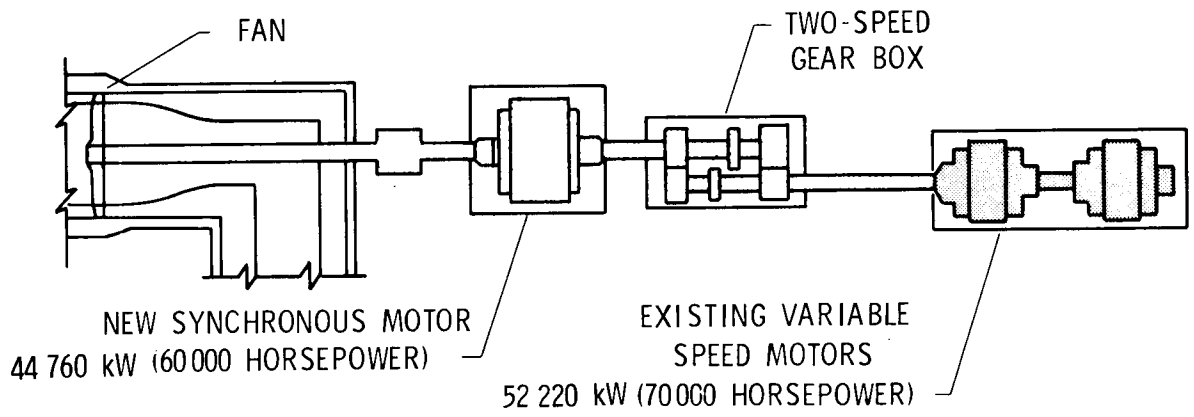


Figure 13.- Schematic of National Transonic Facility drive system.

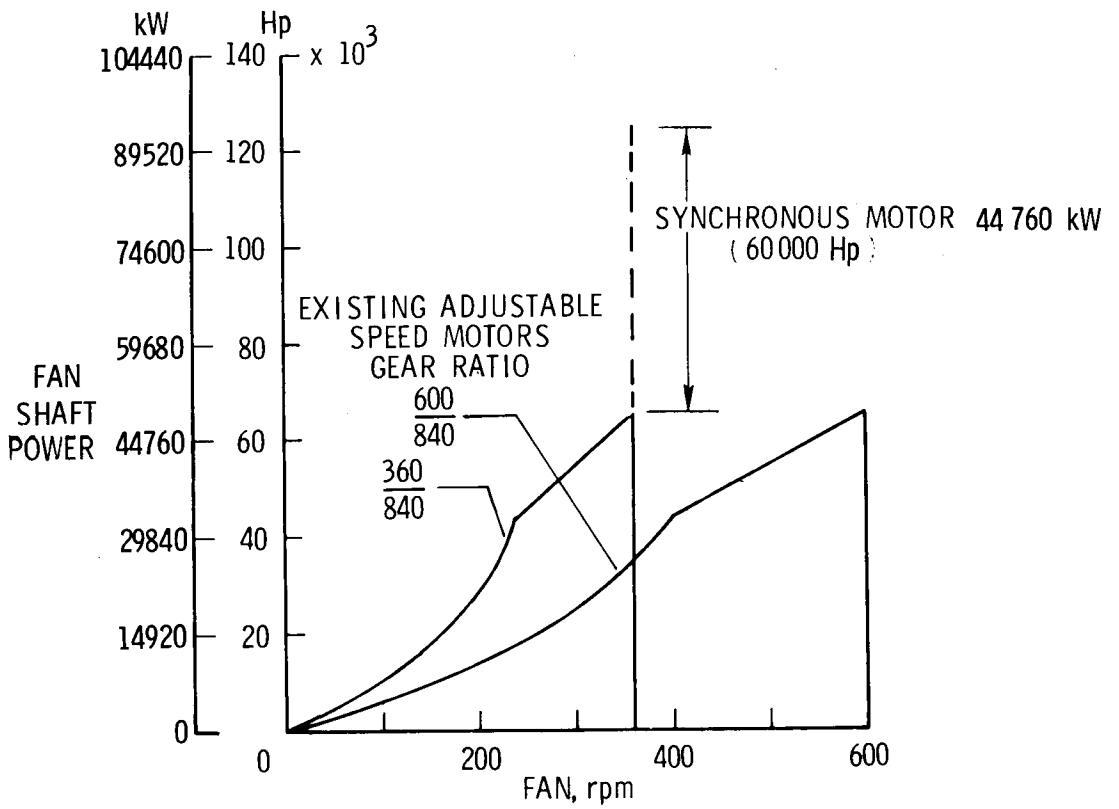


Figure 14.- NTF drive system horsepower available as a function of drive fan rpm.

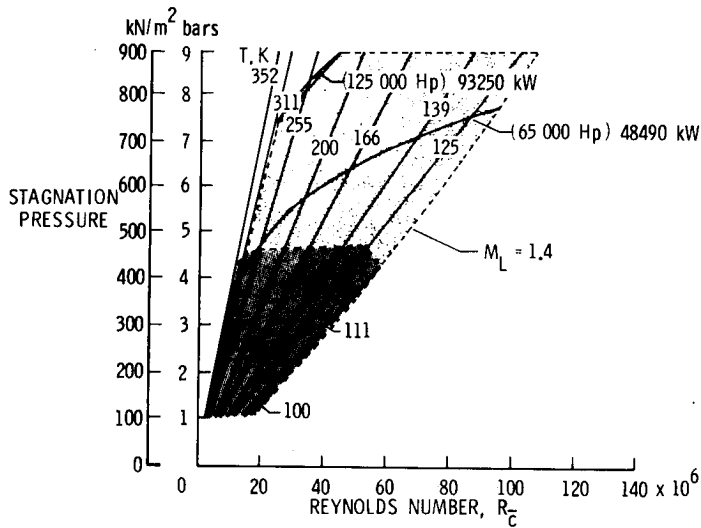


Figure 15.- NTF operating envelope in terms of operating pressure, temperature, and Reynolds number for a Mach number of 0.8.

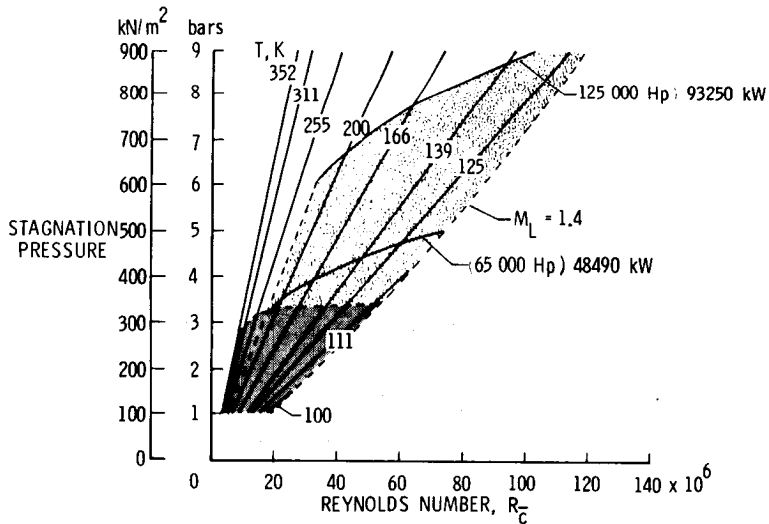


Figure 16.- NTF operating envelope in terms of operating pressure, temperature, and Reynolds number for a Mach number of 1.0.

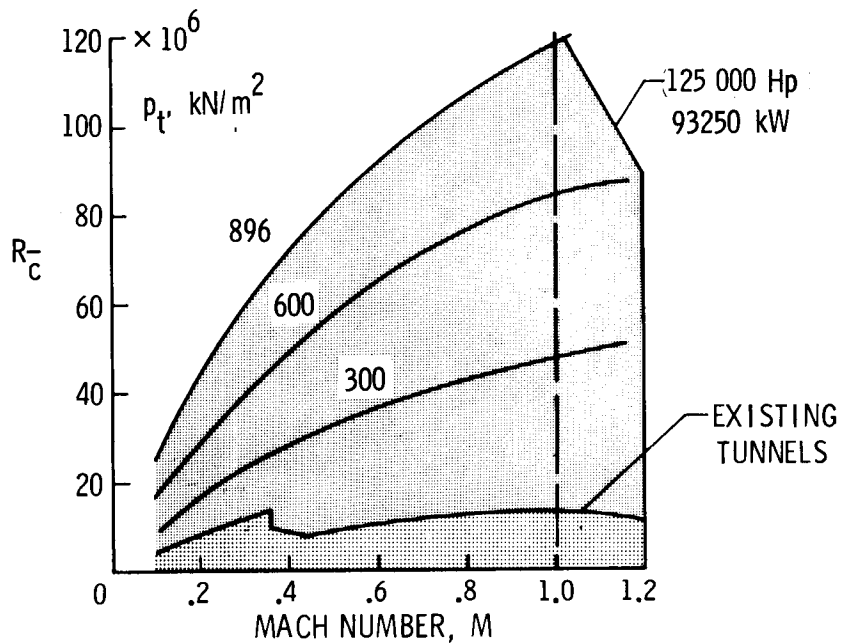


Figure 17.- Maximum Reynolds number as a function of Mach number.

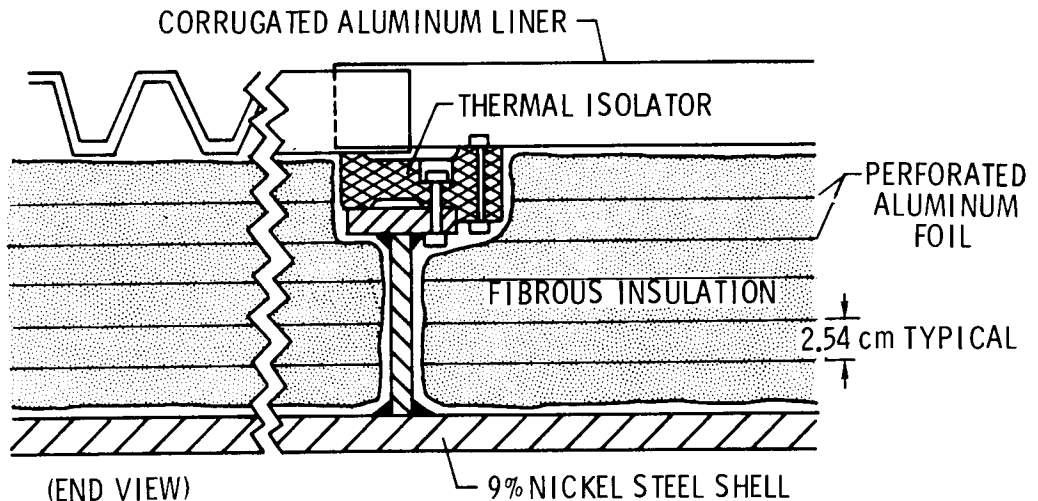


Figure 18.- Sketch showing internal insulation system employing fibrous insulation with interlayered perforated aluminum foil.

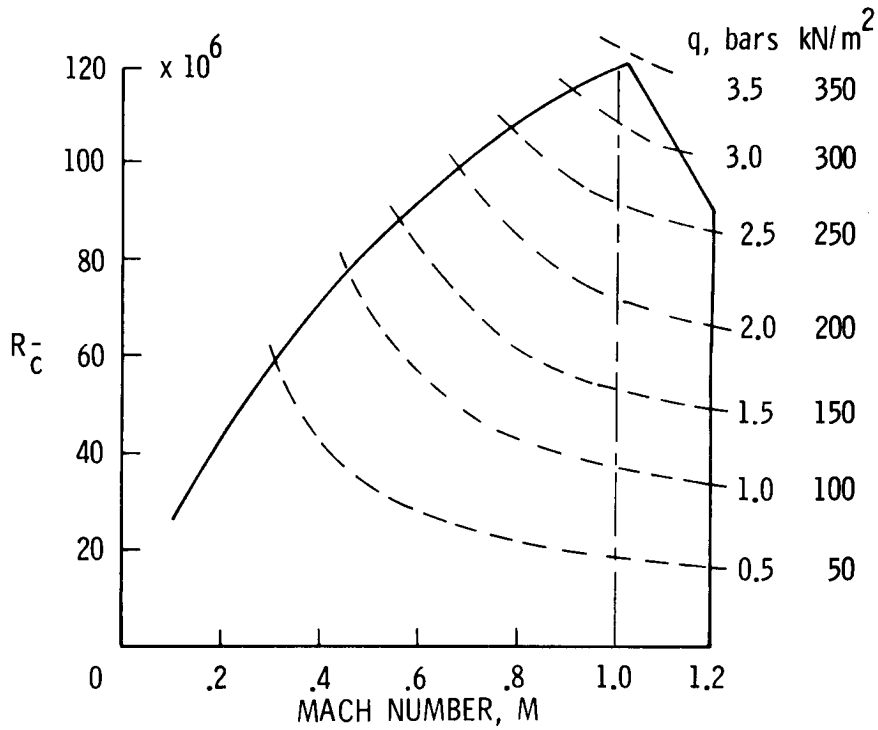


Figure 19.- Maximum Reynolds number envelope with levels of dynamic pressure as a function of Mach number.

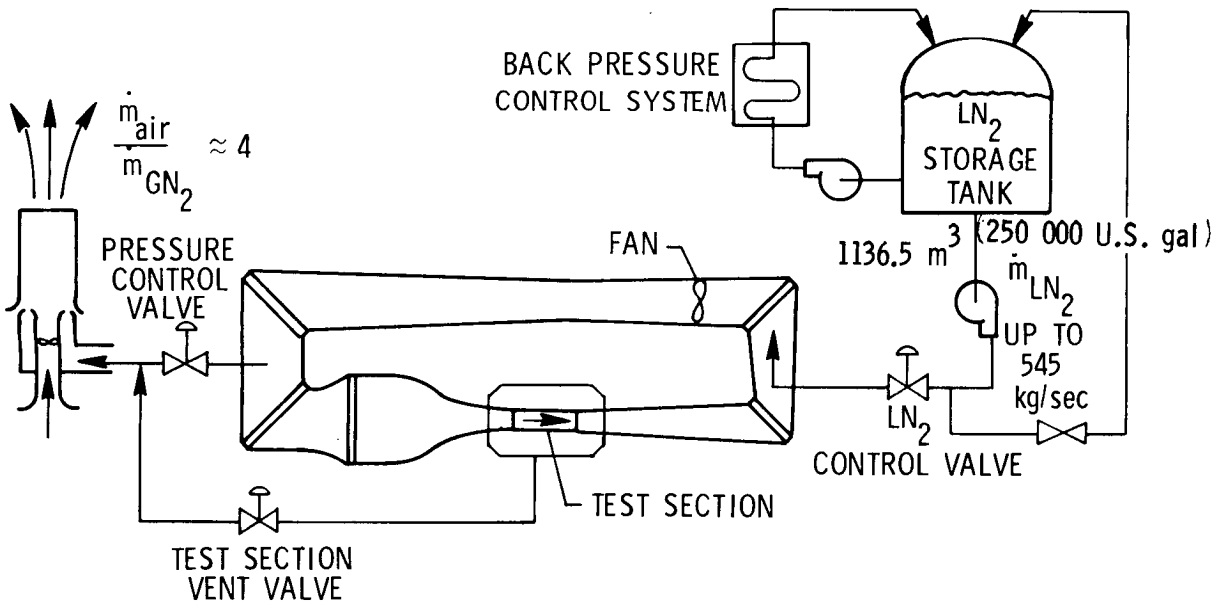
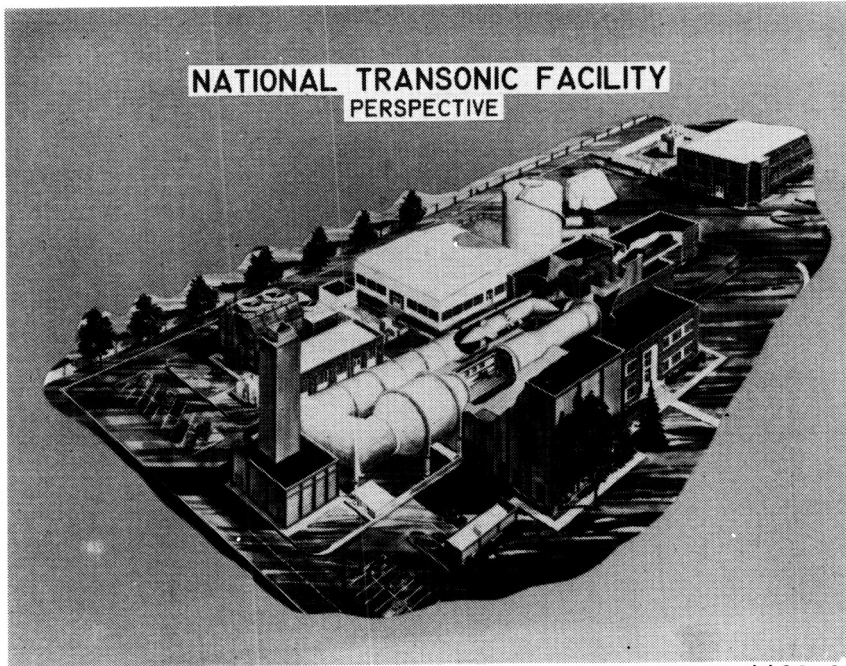


Figure 20.- Schematic of the nitrogen supply and vent system for the NTF.



L-4482-21

Figure 21.- Perspective of the National Transonic Facility.

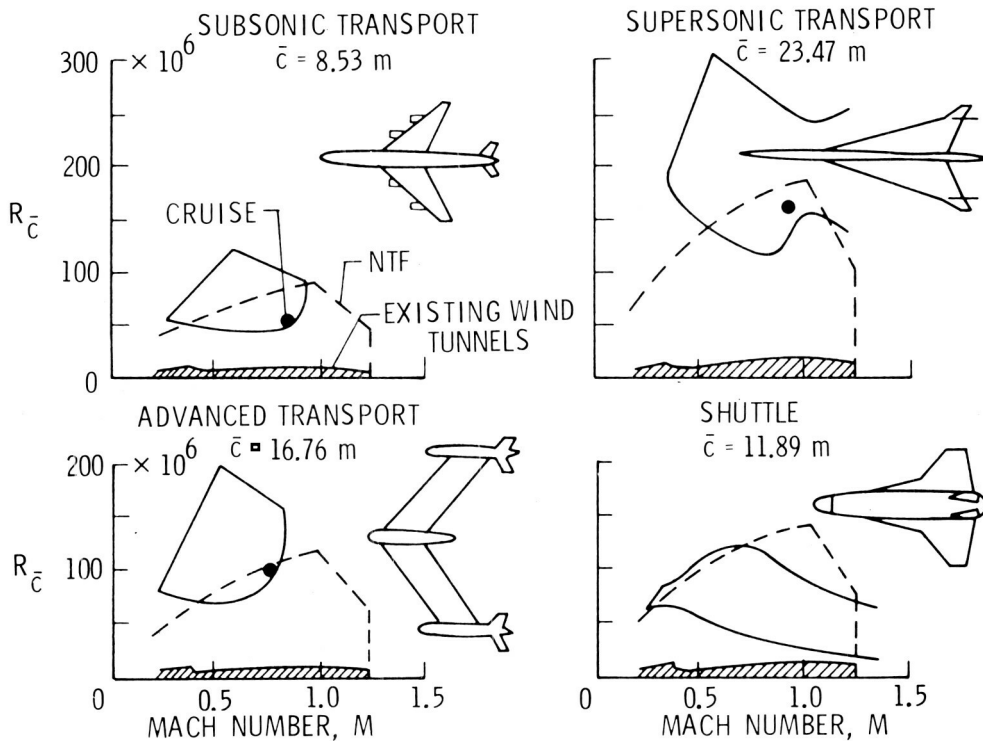


Figure 22.- Comparisons of Reynolds number and Mach number envelopes for full-scale flight vehicles, the NTF, and existing wind tunnels. Typical commercial aircraft.

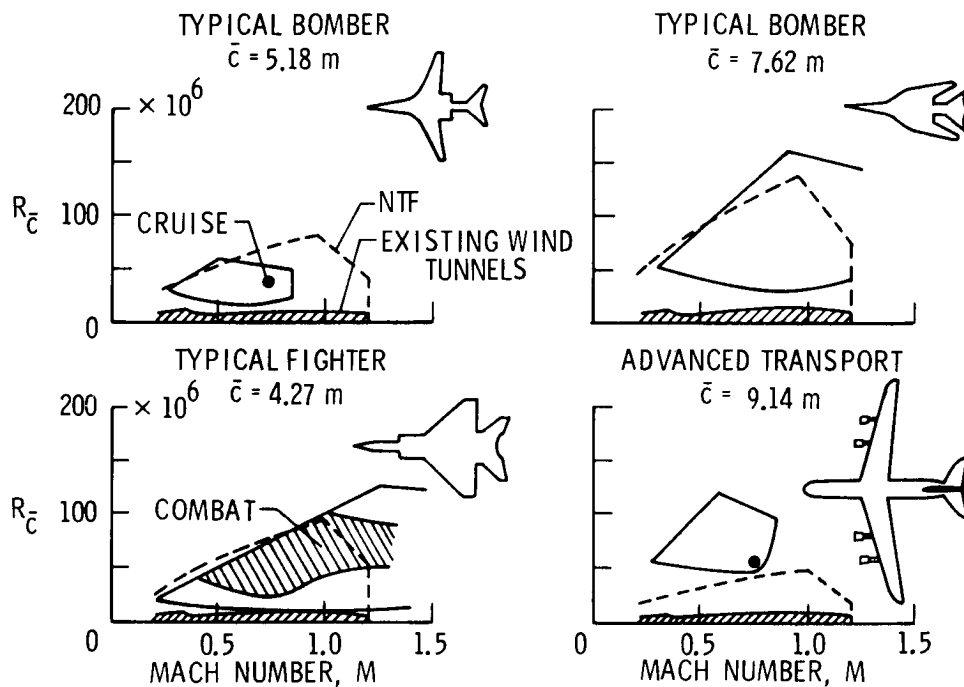


Figure 23.- Comparison of Reynolds number and Mach number envelopes for full-scale flight vehicles, the NTF, and existing wind tunnels. Typical military aircraft.